Journal of Applied Pharmaceutical Science Vol. 14(09), pp 120-127, September, 2024
Available online at http://www.japsonline.com
DOI: 10.7324/JAPS.2024.168308
ISSN 2231-3354

Production and biological properties of nano porous glass microparticles for anticancer drug carrier

Emre Burak Ertuş[1]*, Elif Gulbahce-Mutlu[2], Serife Alpa[2], Abdullah Ozturk[3]

[1]Department of Mechanical Engineering, KTO Karatay University, Konya, Turkiye.
[2]Faculty of Medicine, KTO Karatay University, Konya, Turkiye.
[3]Department of Metallurgical and Materials Engineering, Middle East Technical University, Ankara, Turkiye.

ARTICLE HISTORY

Received on: 26/02/2024
Accepted on: 22/07/2024
Available Online: 05/09/2024

Key words:
Porous glass, 5FU, MCF7, drug release, breast cancer.

ABSTRACT

Nanoporous glass (NPG) microparticles were produced by conventional melt-quenching followed by acid-alkali leaching to get material for anticancer drug carriers. NPG exhibited a positive zeta potential of 34 mV after [3-(2-aminoethylamino) propyl] trimethoxysilane treatment. The specific surface area and the total pore volume of NPG were 47.3 m^2/g and 0.692 cm^3/g, respectively. The 5-Fluorouracil (5FU) loading capacity of NPG was measured as 18.2 ± 0.2 mg_{5FU}/g_{NPG}. The drug release rate was monitored for 120 hours. To evaluate the cytotoxic effects of NPG on both MCF-7 breast cancer cells and MCF-12A, an immortalized cell line, the study employed the 2,3-bis [2-methoxy-4-nitro-5-sulfophenyl]-2H-tetrazolium5-carboxanilide inner salt (XTT) assay. The XTT results revealed that NPG showed a time and concentration-dependent cytotoxic effect. It is anticipated that NPG is a safe and effective material for drug delivery systems for in vitro and a promising alternative material for *in vivo* applications.

INTRODUCTION

Breast cancer accounts for approximately one-tenth of all new cancer diagnoses worldwide. It is the most common type of cancer and one of the leading causes of death in women [1]. The breast cancer cell line MCF-7 and the immortalized cell MCF12A are widely used around the world to carry out research for cancer treatment [2–4]. Although the treatment of breast cancer varies according to the stage of the tumor, it is generally performed in two different ways; local and systemic. While radiotherapy and surgery constitute the local treatment, chemotherapy using anti-cancer drugs is the most commonly used method among the other treatment methods although it affects the whole body and varies from person to person [5]. Anticancer drugs used in chemotherapy have two negative side effects; i) they are used in high doses to achieve chemotherapeutic effect by causing cell toxicity, and ii) tumor cells gain resistance to chemotherapy [6]. Thus, the anticancer drug does not show the expected effect on tumor cells and causes the progression of the disease. As a result, success in cancer treatment will be hindered.

5-Fluorouracil (5FU) is a pyrimidine analog widely used in cancer chemotherapy. The clinical use of 5FU began in 1957. It has been accepted as a highly effective agent against tumor development since then. It prevents deoxyribonucleic acid (DNA) synthesis by inhibiting the thymine nucleotide in the DNA structure and ribonucleic acid synthesis by inhibiting the phosphate enzyme. Nowadays, it is commonly used in the treatment of many cancer types such as breast, colon, rectum, ovarian, stomach, brain, pancreatic, and skin cancer [7,8].

The toxic character of the cancer drugs causes undesirable effects on the digestive system, nervous system, skin, and heart. In recent years, controlled drug release studies based on porous materials have gained importance due to the advantages such as maintaining the drug level at a therapeutic rate and minimizing the side effects [9]. In controlled drug release studies, loading drugs into porous materials is one of the most frequently used ways for drug delivery. It is known that the drug release rate can be controlled depending on the

*Corresponding Author
Emre Burak Ertuş, Department of Mechanical Engineering, KTO Karatay University, Konya, Turkiye. E-mail: burak.ertus @ karatay.edu.tr

porosity and permeability of the drug carrier material [10]. Extensive studies were performed on controlled drug release by loading 5FU into different nanoparticles [11–13] and the cytotoxic effect on the MCF-7 cell line [14–16]. However, a systematic study on the utilization of a nanoporous glass (NPG) as a 5FU anticancer drug carrier is nonexistent.

NPG is an amorphous material containing nanometer or micrometer size of pores, high surface area, and high (~35%) pore volume. It shows high chemical stability against organic solvents and strong acids (except HF). Its surface structure, suitable for easy functionalization, allows NPG to be grafted with bioadhesive or biotargetable molecules [17,18]. NPG differs from other porous materials in drug delivery due to its advantages including low production cost and suitability for mass production [18,19]. The physical properties of NPG including pore size, pore volume, and surface area can be easily tailored by selecting different production process parameters. Due to its unique characteristics, NPG attracts attention as a promising new-generation material in biological applications. Mazilu *et al.* [20] reported that osteoblast cells showed viability and proliferation on and in NPG and, the glucose oxidase enzyme loaded into the glass showed enzymatic activity. Li *et al.* [21] produced NPG microspheres loaded with biological molecules such as dextran-70. The results revealed that biological molecules can fill the nanochannels in NPG and allow controlled release within the tumor.

The purpose of this study was to investigate the possibility of the utilization of NPG as a 5FU anticancer drug carrier. The 5FU loading capacity and drug release kinetics of NPG was researched. The cytotoxic effect of this drug system on MCF7 and MCF12A cell lines was elucidated. To the best of the authors' knowledge, the findings reported in this manuscript have been publicized in the open literature for the first time.

MATERIALS AND METHODS

Materials

High-purity SiO_2 (Eczacıbaşı, Türkiye), Na_2CO_3 (Merck, USA), H_3BO_3 (Eti Maden, Türkiye), and $Al(OH)_3$ (Eti Alüminyum, Türkiye) powders served as the initial chemical constituents for glass production. [3-(2-aminoethylamino) propyl] trimethoxysilane (technical grade, ≥80% Sigma-Aldrich), toluene (anhydrous, 99.8%, Sigma-Aldrich), NaOH (ACS reagent pellets, Merck), 5FU, (≥99% powder, Sigma), and HCl (%37 solution, Sigma-Aldrich) were used for NPG modification and functionalization. The materials used for cell culture and 2,3-bis [2-methoxy-4-nitro-5-sulfophenyl]-2H-tetrazolium5-carboxanilide inner salt (XTT) assay are phosphate buffered saline solution (Ph 7.4, Sigma) MCF7 breast cancer cell line (ATCC® HTB-22™ American type culture collection, USA), RPMI-1640 medium (BioChrom, Germany), fetal bovine serum (FBS, Biological Industries, Sigma-Aldrich, Italy), MCF-12A cell line (ATCC® CRL-10782™), DMEM-high glucose medium (ThermoFischer, Waltham, USA), gentamicin sulfate solution (Sigma-Aldrich, Italy), Trypsin-EDTA (0.05%, Gibco™ ThermoFischer, USA), XTT assay kit (Biological Industries Ltd., Israel), epidermal growth factor (EGF, Roche), hydrocortisone (Sigma-Aldrich), human insulin solution (Sigma-Aldrich), and MEM non-essential amino acids solution (Gibco™, ThermoFischer, USA).

NPG preparation

A sodium borosilicate glass was produced using a conventional melt-quenching method similar to our previous study, with the specified composition of $58SiO_2$-$31.6B_2O_3$-9Na2O-$1.4Al_2O_3$ (by weight percent) [22]. Batches were formed by mixing the necessary amount of each ingredient (SiO_2, Na_2CO_3, H_3BO_3, and $Al(OH)_3$ powders). The mixture was melted in a 90Pt-10Rh crucible in an electric furnace at 1300°C in the air for 30 minutes. Then, the melt was air quenched. The resulting glass shards were further crushed using a mortar with a pestle and re-melted in the same crucible at 1400°C for 1 hour to ensure chemical homogeneity. Following the melting process, the glass melt was cast onto a polished stainless-steel plate. Glass pieces were heat treated at 550°C for 12 hours. Then, the soluble alkali-rich borate phase was removed by acid leaching process carried out at 1M HCl solution at 90°C for 24 hours. The glass was treated with 0.5M NaOH solution at room temperature for 6 hours to remove the silica colloids that remained inside the pores formed after acid leaching. After acid and alkali treatments, the glass was washed with distilled water for 24 hours. The remaining NPG was dried at 90°C for 24 hours, pulverized in an agate mortar with a pestle, and sieved to the size of less than 37 μm (400 mesh).

To functionalize the NPG surface with amine groups, a 0.2 g NPG was mixed with 1 ml [3-(2-aminoethylamino) propyl] trimethoxysilane and 5 ml anhydrous toluene. Then, the mixture was refluxed at 110°C for 24 hours under constant stirring. After cooling down to room temperature, NPG was separated from the solution by centrifugation at 4,500 rpm for 1 hour, and washed with toluene and methyl alcohol. Finally, it was dried in an oven at 80°C for 24 hours.

NPG characterization

The average particle size of NPG was measured by laser diffraction technique using a Malvern Mastersizer 2,000. The Zeta potential of NPG was measured in distilled water with Malvern Nano ZS90 at 25°C. Field emission scanning electronic microscopy (FESEM, ZEISS GeminiSEM 500) was employed to examine the surface and pore morphology. Nitrogen physisorption measurements were carried out to examine the porosity of NPG using the Quantachrome Autosorb-6 instrument. The specimen was degassed at 100°C for 3 hours. The specific surface area of NPG was measured based on the Brunauer–Emmett–Teller (BET) analysis and the total pore volume (V_p) was calculated from the adsorption data at the maximum relative pressure (P/P_o). The pore size distribution was measured from the desorption branch of the isotherm using the BJH model.

5 FU load and release

A 5FU/Phosphate Buffer Solution (PBS, pH:7.4) at a concentration of 3 mg/ml was used for the 5FU loading medium. 30 mg of NPG was incubated in 5 ml of solution with a stirring speed of 500 rpm for 24 hours. Then, 5FU loaded NPG (NPG@5FU) was separated from the solution by centrifugation

twice at 4,500 rpm and dried at 60°C for 2 hours. The absorbance of the supernatant was measured at a wavelength of 266 nm using a UV-Vis spectrophotometer (Agilent, Cary60). The 5FU loading capacity of NPG was calculated by the following equation:

$$C_L = \frac{(C_i - C_f) \times V}{\text{m}} \quad (1)$$

where C_i (mg/ml) is the initial solution concentration, C_f (mg/ml) is the solution concentration after loading, V (ml) is the solution volume, and m (g) is the amount of NPG in the solution.

The 5FU release profile was determined by adding 10 mg of NPG@5FU into 20 ml of PBS solution. Release experiments were carried out under a constant stirring speed of 500 rpm at 37°C. 2 ml aliquots were taken from the solution at regular intervals and centrifuged at 4,500 rpm. The absorbance of 1 ml supernatant was measured using a UV-Vis spectrophotometer at 266 nm wavelength. 1 ml precipitate with NPG@5FU particles was redispersed and added back to stock solutions. The amount of 5FU released (C_R) was calculated by the following equation:

$$C_R = \frac{C_t V_t + C_{t\text{-}1}}{\text{m}} \quad (2)$$

where C_t (mg/ml) is the concentration of the sample taken at the specified release time, V_t (ml) is the volume of solution at time t, and m (g) indicates the amount of NPG@5FU in the solution. Release experiments were repeated for three cycles. The data points were obtained by taking the mean average of the three values to get a reliable value for each drug release. 5FU release behavior was investigated according to the kinetic models specified below:

First order: $C_t = C_{max}(1\text{-}\exp(-k_1.t))$ (3)

Korsmeyer-Peppas: $C_t = k_{km}.t^n$ (4)

where C_t indicates the amount of drug release at the time of t, C_{max} indicates the maximum amount of drug release, k_1, k_{km}, and n are the constants obtained after fitting [23,24]. Well-fitted ($R > 0.99$) calibration curve of 5FU standard solutions was used for load and release calculations.

Cell culture

The study protocol was approved by the Ethics Committee of KTO Karatay University Non-Pharmaceutical and Medical Device Research Ethics Committee (Decision No. 2020–016, dated 22.05.2020). The MCF7, breast cancer cells, and MCF12A, immortalized human cells, were used in this study.

The MCF7 breast cancer cell line (estrogen-dependent epithelial cell line) was maintained in RPMI-1640 medium supplemented with 10% FBS and 0.1% gentamicin sulfate solution. This formulation provided the necessary nutrients and antibiotics for optimal growth and culture stability. Concomitantly, the MCF12A cell line, which exhibits characteristics of normal human mammary epithelial cells, was cultured in a DMEM-high glucose medium. This nutrient-rich medium was enhanced with 10% FBS (fetal bovine serum), 0.1% pen-strep (penicillin-streptomycin), 1% NEAA (non-essential amino acids), and specific growth factors: 20 ng/ml of EGF (epidermal growth factor], 500 ng/ml of hydrocortisone, and 0.01 mg/ml human insulin. This combination facilitated proliferation and maintained the phenotype of MCF12A cells [25].

Frozen MCF7 and MCF12A cells were rapidly thawed in a water bath at 37°C for 1–2 minutes. The cells were immediately transferred to a 15 ml tube containing medium in the laminar flow cabinet after that centrifuged at 1,000 rpm for 5 minutes. After the centrifuge, the supernatant was removed. Then, they were transferred to the T25 flask. The flasks were placed in a 5% CO_2 and 37°C incubator. For the next passage, the confluence of cells was observed every 2 days, and the medium was changed every 2–3 days. Both cell lines were also subcultured weekly using 0.02% EDTA and 0.05% trypsin.

MCF7 and MCF12A cells were seeded at a density of 2 × 104 cells/well in 96 well plates and were incubated at 37°C in 5% CO_2 for 24 hours. Cells were then treated with 5FU, NPG, and NPG@5FU of varying concentrations (500, 50, and 25 µg/ml) in triplicate, and incubated for 24, 48, and 72 hours. At the end of these periods, images of cells in all experimental groups were taken with the help of a trinocular inverted microscope (Nicon, Japan). NPG and NPG@5FU were sterilized under UV light for 3 hours before the addition to the cell medium. A positive control of untreated cells was included. Finally, cell count and cell viability analyses were performed.

XTT assay

The cell proliferation was determined by using a standard 2,3-bis [2-methoxy-4-nitro5-sulfophenyl]-2H-tetrazolium5-carboxanilide inner salt (XTT) assay kit. The kit is based on the proliferation of living cells by forming an orange soluble formazan dye of tetrazolium salt, mostly due to mitochondrial dehydrogenase activity. After 24, 48, and 72 hours incubation of cells with NPGs, plates were read at 490 nm using a UV-Vis Spectrophotometer (Multiskan Sky Microplate, Thermo Fisher Scientific, Waltham, Massachusetts, ABD). All concentrations were repeated 3 times in each assay.

Statistical analysis

Statistical analysis was conducted using GraphPad Prism 9.2.0. IC50 values were determined by the nonlinear regression graph of the OD values obtained according to time. Multiple group comparisons were analyzed by two-way ANOVA and Bonferroni post hoc test. Differences between two means with $p < 0.05$ were considered significant (*).

RESULTS AND DISCUSSION

Characterization of NPG

The size distribution histogram of NPG particles is shown in Figure 1. The size of the particles varies in the range from 0.8 to 61 µm. The volume-weighted average particle size was 8.7 µm. A small amount (~4%) of particles with a particle size bigger than 37 µm passed through the sieve due to the orientation of the elongated particles and the deformation of the sieve wires over time.

NPG has a negative surface charge and slightly acidic character due to silanol (Si-OH) groups on its surface [26].

As shown in Figure 2, the surface charge of NPG (−21 mV) became positive (34.7 mV) after treatment of the surface with positively charged -NH_2^+ groups. The finding verifies that the surface functionalization process is successful. Similar results were reported by Dau *et al.* [27].

SEM images taken from the surface of NPG at 50,000X and 100,000X are presented in Figure 3. NPG has a characteristic interconnected pore structure [17,28]. No significant change in the pore structure was observed due to the functionalization process.

The N_2 adsorption–desorption isotherm of NPG is given in Figure 4(a). The pore structure defines the isotherm shape. NPG has type IVa isotherm according to IUPAC classifications. A combination of H1 and H2 type hysteresis curves due to pore blocking/percolation or evaporation caused by cavitation has been observed in materials with a narrow pore size (ink-bottle pore model) [29].

The pore size distribution graph of NPG, shown in Figure 4(b), reveals that the maximum around 30 nm belongs to interconnected pores in the silica-rich skeleton formed by the dissolution of the sodium-borate phase of the glass structure and called primary pores. The hump between 2 and 4 nm belongs to the pores formed by the dissolution of a small amount of silica from the sodium-borate phase into the acidic solution and precipitation as silica clusters in the primary pores, so-called secondary pores. The specific surface area and the pore volume values as calculated from N_2 adsorption–desorption analysis were 47.3 m^2/g and 0.692 cm^3/g, respectively. The functional groups cover the silica clusters and partially close the secondary pores [13,30]. This is the reason why the values for the pore volume of secondary pores and specific surface area were less than that for the other porous glasses [22].

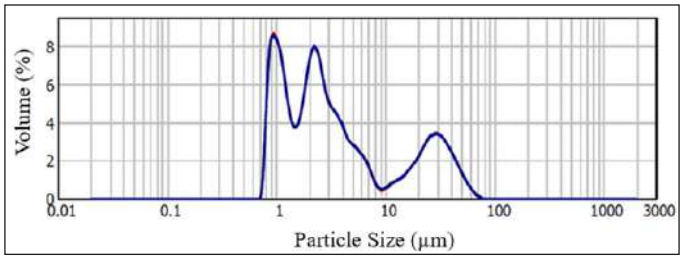

Figure 1. Particle size distribution histogram of NPG.

The 5FU loading capacity of NPG was calculated as 18.2 ± 0.2 mg_{5FU}/g_{NPG}. The drug loading capacity of NPG was lower than similar porous nano-sized silicas [13,14,30–32]. The large particle size (>1 μm) of NPG is the main reason for the comparatively low loading rate. It is believed that the entangled pore structure prevents the drug diffusion into the center of NPG and the drug solution cannot reach the pores in the inner parts of NPG sufficiently.

The 5FU release profile of NPG@5FU is shown in Figure 5. A burst release of around 65% takes place within 3 hours. This instantaneous release is attributed to 5FU molecules located on the surface and the external pores of NPG, which get rid of the pores more easily and pass into the solution. The amount of release continues to increase, reaching around 80% at the end of the 12th hour, and continues at this level until 120 hours. The release profiles were well-fitted in Korsmeyer–Peppas (R^2 = 0.97) and first-order (R^2 = 0.98) kinetic models.

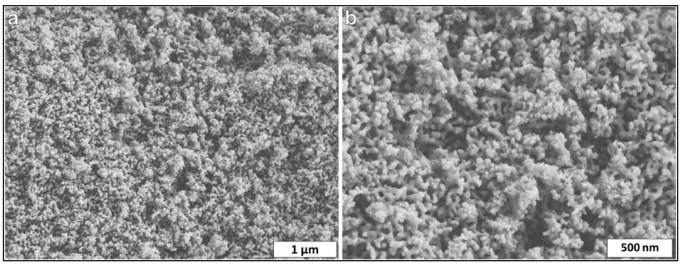

Figure 3. SEM images taken from the surface of NPG at (a) 50,000X and (b) 100,000X.

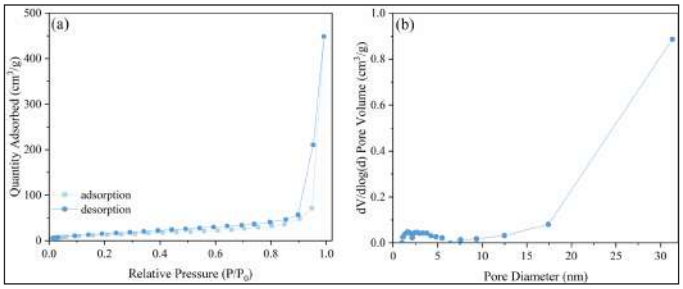

Figure 4. (a) Nitrogen adsorption–desorption isotherm and (b) corresponding pore size distribution of NPG.

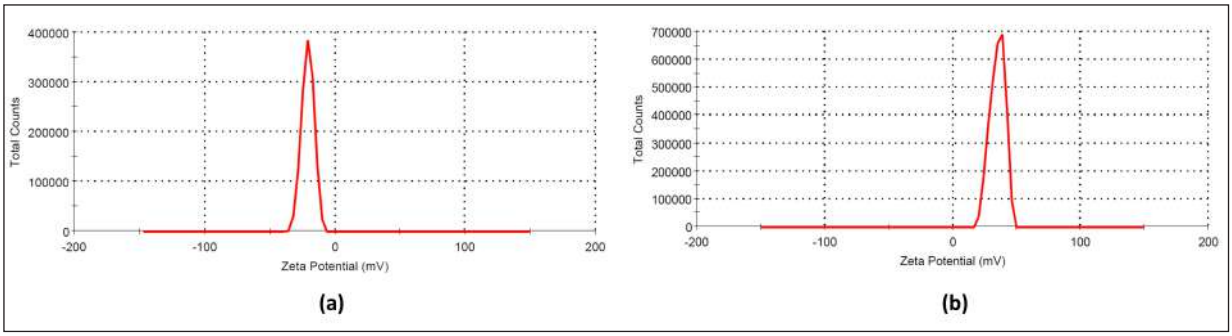

Figure 2. Zeta potential of NPG (a) before and (b) after surface functionalization.

The first-order kinetic model describes the drug release process as dependent on the drug concentration that can be loaded into the porous material. The maximum amount of drug release (C_{max}) and rate constant calculated according to the kinetic model were 78.2% ± 2.4% and 0.42 h^{-1}, respectively**.** The Korsmeyer–Peppas model is based on a diffusion-based process. The exponent *n* in the kinetic model is the diffusion exponent that defines the release mechanism. If $n < 0.5$, the release depends on Fickian diffusion. That is, it depends on the average free path that the drug molecules will travel in the porous structure. It points out that the diffusion of drug molecules through the pores is largely dependent on the interaction of the drug molecule with the pore walls. Exponent n of about 0.05 confirms that the Fickian diffusion is the controlling factor in drug release.

Morphologic changes of MCF7 and MCF12A cells after treatment

To reveal the effect of 5FU and NPG on MCF7 and MCF12A cell morphology, culture cell line images were taken after 24, 48, and 72 hours were evaluated. The images taken via an optical microscope are shown in Figures 6 and 7.

MCF7 cells in the control group shown in Figure 6(a) did not exhibit any significant morphological changes. MCF7 cells after treatment with 5FU were smaller and separated from each other. In addition, the cell membranes were rough and relatively darker as shown in Figure 6(b). The NPG-treated cells shown in Figure 6(c) were mostly adhered to each other and there were few cells floating in the medium. For the culture treated with NPG@5FU shown in Figure 6(d), cells were mostly round and smaller, although there were some cells with adherent and smooth membranes. In addition, there was abundant cell debris in the medium. Similar morphologies were observed for the cells in the application groups that had different dosages and different treatment periods.

The NPG-treated MCF12A cells shown in Figure 7(c) displayed similar morphology to the cells in the control group as shown in Figure 7(a). The cells treated with 5FU shown in Figure 7(b) were separated from each other and their membranes were rough and not bright. The membranes of the cells treated with NPG@5FU as shown in Figure 7(d) were shiny, partially separated from each other, and some were reduced in size. Similar morphologies as mentioned above were observed for the cells in the application groups that had different dosages and different treatment periods.

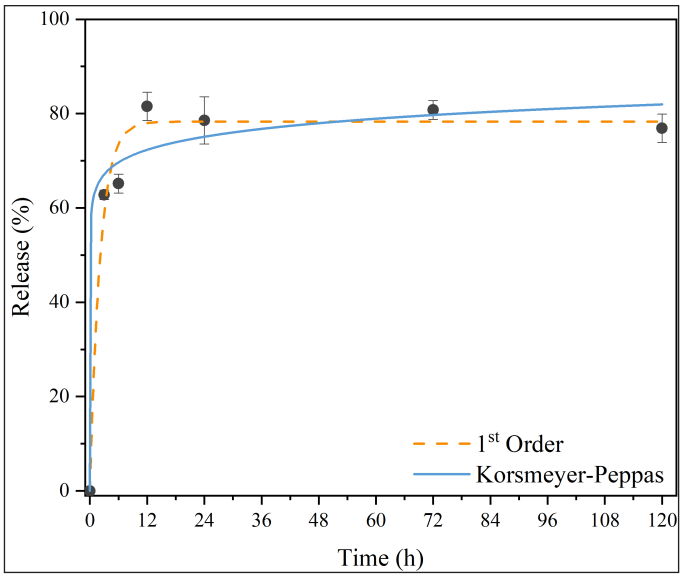

Figure 5. 5FU release kinetics of NPG@5FU.

Cytotoxicity assay on MCF7 and MCF-12A cells

2,3-bis (2-methoxy-4-nitro-5-sulfophenyl)-5-[(phenylamino) carbonyl]-2H-tetrazo-lium hydroxide (XTT) assay that measures the metabolic activity of viable cells was used to assess the cytotoxicity of NPG in vitro. XTT cytotoxicity assay of 5FU, NPG, and NPG@5FU administered at various concentrations (500, 50, and 25 µg/ml) in MCF7 cells were presented in Figure 8.

For 24 hours, the NPG@5FU concentration that reduces cell viability by 50% (IC50) for the MCF7 cell line was calculated as 11.89 µg/ml, whereas the IC50 NPG@5FU concentration for the MCF12A cell lines was 27.25 µg/ml. After 48 hours, the NPG@5FU anti-proliferative effect was prominent in MCF7 cells with an IC50 rate of 11.34 µg/ml. In MCF12A cells, the IC50 was 20.08 µg/ml according to the XTT results after 48 hours of application. After 72 hours of

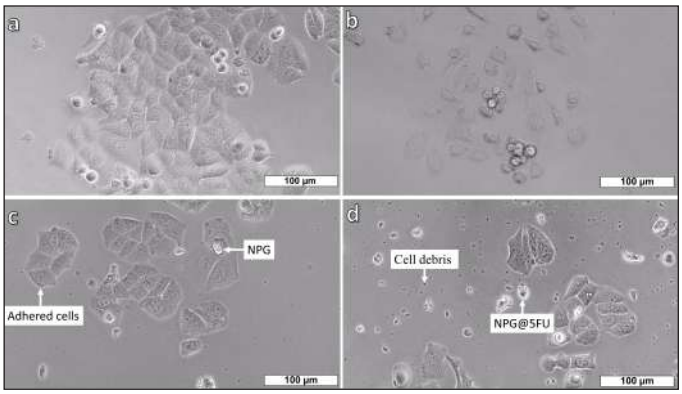

Figure 6. MCF7 cell line images (a) control, after treatments with (b) 500 µg/ml 5FU, (c) 500 µg/ml NPG, and (d) 500 µg/ml NPG@5FU for 24 hours.

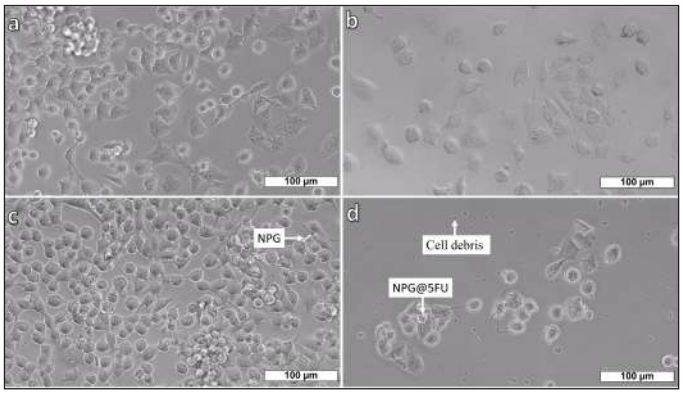

Figure 7. MCF12A cell line images (a) control, after treatments with (b) 500 µg/ml 5FU, (c) 500 µg/ml NPG, and (d) 500 µg/ml NPG@5FU for 24 hours.

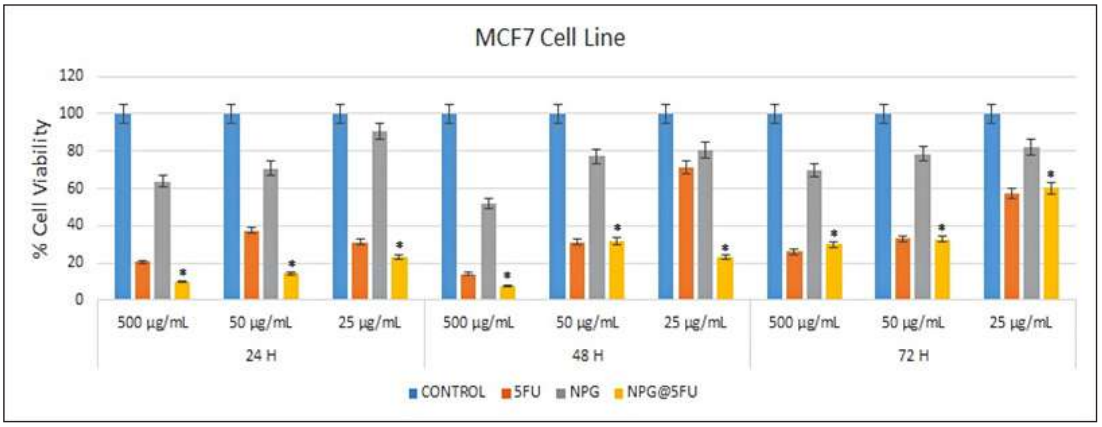

Figure 8. XTT cytotoxicity assay of 5FU, NPG, and NPG@5FU was administered at various concentrations (500, 50, and 25 µg/ml) in MCF7 cells.

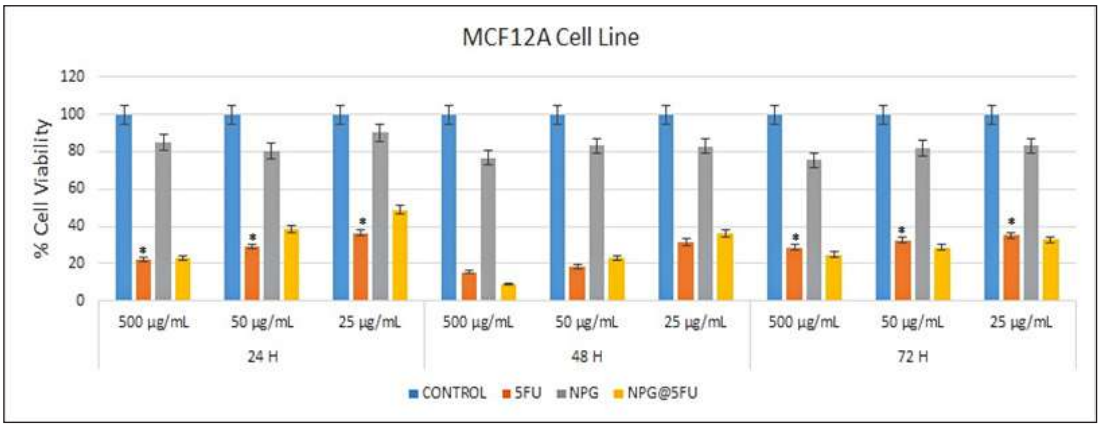

Figure 9. XTT cytotoxicity assay of NPG and 5FU-loaded NPGs administered at various concentrations (500, 50, and 25 µg/ml) in MCF12A cells.

treatment, the XTT results of MCF7 and MCF12A cell lines showed that the NPG@5FU IC50 values were 28.61 and 22.75 µg/ml, respectively (p <0.001).

It was noted that NPG@5FU had lower cell viability than NPG application groups in the MCF7 cell line. Most importantly, it exhibited significantly lower cell viability compared to treatments with either NPG or 5FU individually. In addition, this activity varied depending on the dose and time, and the effect of NPG on cell viability increased at decreasing concentrations. For example, at the highest dose of 500 µg/ml, for 24 hours 5FU and NPG showed 20.6% and 63.84% cell viability, respectively, while NPG@5FU showed 10.3%. At the lowest dose of 25 µg/ml, 5FU and NPG showed 31.33% and 90.57% cell viability, respectively, while NPG@5FU showed 23.24%.

For 48 h, similar results were obtained at the dose of 500 µg/ml over a 24-h period. At the dose of 50 µg/ml, 5FU and NPG@5FU showed close cell viability, 31.19% and 31.76%, respectively. However, the cell viability (71.33%) in the 5FU group at the dose of 25 µg/ml was significantly higher than the NPG@5FU cell viability (23.24%). In 72 hours, the cell viability of both 5FU and NPG@5FU at doses of 500 and 50 µg/ml is close to each other. However, at the dose of 25 µg/ml, the cell viability of the 5FU group was 33.06% and that of the NPG@5FU group was 32.72%. The finding proves that the 25 µg/ml dose increased cell viability compared to the other groups.

The XTT cytotoxicity assay of NPG and 5FU-loaded NPG administered at various concentrations (500, 50, and 25 µg/ml) in MCF12A cells were presented in Figure 9. Both 5FU and NPG@5FU at the dose of 500 µg/ml in the MCF12A cell line showed close cell viability, 22.06% and 23.12%, respectively. In 48 hours, 5FU at the dose of 500 µg/ml showed 15.15% cell viability, while NPG@5FU showed 17.06% cell viability. The cell viability of the NPG@5FU group was higher than that of the 5FU group at decreasing doses in both periods. After 72 hours of application, 5FU and NPG@5FU showed almost similar cell viability at all doses. While a lower cell viability was observed at the highest dose of 500 µg/ml, a higher cell viability was determined at the lowest dose of 25 µg/ml. The cytotoxicity of NPG in MCF12A cells was almost negligible at periods and doses administered, suggesting that NPG is well tolerated in the MCF12A cell line.

CONCLUSION

NPG microparticles are produced by successive acid and alkaline treatments conducted on a sodium borosilicate glass. A release of 78.2% of the drug in PBS medium is realized as NPG with an average particle size of 8.7 μm was loaded with 5FU up to 18.2 ± 0.2 mg_{5FU}/g_{NPG}. First-order and Korsmayer–Peppas kinetic models are suitable to describe the drug release regime. Although there were cells that died in the early culture period of MCF7 cell lines treated only with 5FU, the surviving cells eventually multiplied within 48–72 hours of culture periods. This indicates that the effect of 5FU on cells diminishes over time. However, it has been observed that dose- and time-dependent cytotoxicity is more prominent for the NPG@5FU group. The main reason for this seems to be the continuous release of 5FU, sustaining its dose and time-dependent effect at 24, 48, and 72 hours of culture. This observation supports the idea that drug carrier-based sustained-release formulations might effectively enhance the therapeutic agent's efficacy by inducing apoptosis. The cytotoxicity of NPG in MCF12A cells was almost negligible for all periods and doses processed suggesting that NPG is well tolerated in this cell line. The drug-loaded NPG can be a promising material to minimize both drug resistance and side effects of high-dose anticancer drugs. NPG is a safe and effective material for drug delivery systems in vitro and has a potential for *in vivo* applications.

ACKNOWLEDGMENTS

The authors thank The Scientific and Technological Research Council of Turkey (TÜBİTAK) for the partial financial support through project no: 120M929.

AUTHOR CONTRIBUTIONS

All authors made substantial contributions to conception and design, acquisition of data, or analysis and interpretation of data; took part in drafting the article or revising it critically for important intellectual content; agreed to submit to the current journal; gave final approval of the version to be published; and agree to be accountable for all aspects of the work. All the authors are eligible to be an author as per the International Committee of Medical Journal Editors (ICMJE) requirements/guidelines.

CONFLICTS OF INTEREST

The authors report no financial or any other conflicts of interest in this work.

ETHICAL APPROVALS

The study protocol was approved by the Health Ethics Research Committee of KTO Karatay University Non-Pharmaceutical and Medical Device Research Ethics Committee (Decision No. 2020–016, dated 22.05.2020). The MCF7, breast cancer cells, and MCF12A, immortalized human cells, were used in this study.

DATA AVAILABILITY

All data generated and analyzed are included in this research article.

USE OF ARTIFICIAL INTELLIGENCE (AI)-ASSISTED TECHNOLOGY

The authors declares that they have not used artificial intelligence (AI)-tools for writing and editing of the manuscript, and no images were manipulated using AI.

PUBLISHER'S NOTE

All claims expressed in this article are solely those of the authors and do not necessarily represent those of the publisher, the editors and the reviewers. This journal remains neutral with regard to jurisdictional claims in published institutional affiliation.

REFERENCES

1. Jemal A, Bray F, Center MM, Ferlay J, Ward E, Forman D. Global cancer statistics. CA Cancer J Clin. 2011;61(2):69–90.
2. Soule H, Vazquez J, Long A, Albert S, Brennan M. A human cell line from a pleural effusion derived from a breast carcinoma. J Natl Cancer Inst. 1973;51(5):1409–16.
3. Nugoli M, Chuchana P, Vendrell J, Orsetti B, Ursule L, Nguyen C, *et al.* Genetic variability in MCF-7 sublines: evidence of rapid genomic and RNA expression profile modifications. BMC Cancer. 2003;3(1):1–12.
4. Paine TM, Soule HD, Pauley RJ, Dawson PJ. Characterization of epithelial phenotypes in mortal and immortal human breast cells. Int J Cancer. 1992;50(3):463–73.
5. Waks AG, Winer EP. Breast cancer treatment: a review. Jama. 2019;321(3):288–300.
6. Szakács G, Paterson JK, Ludwig JA, Booth-Genthe C, Gottesman MM. Targeting multidrug resistance in cancer. Nat Rev Drug Discov. 2006;5(3):219–34.
7. Diasio RB, Harris BE. Clinical pharmacology of 5-fluorouracil. Clin Pharmacokinet. 1989;16(4):215–37.
8. Ghoshal K, Jacob ST. An alternative molecular mechanism of action of 5-fluorouracil, a potent anticancer drug. Biochem Pharmacol. 1997;53(11):1569–75.
9. Dhankhar R, Vyas SP, Jain AK, Arora S, Rath G, Goyal AK. Advances in novel drug delivery strategies for breast cancer therapy. Artif Cells Blood Sub Biotechnol. 2010;38(5):230–49.
10. Arruebo M. Drug delivery from structured porous inorganic materials. Wiley Interdiscip Rev Nanomed Nanobiotechnol. 2012;4(1):16–30.
11. Gârea S, Mihai A, Ghebaur A, Nistor C, Sârbu A. Porous clay heterostructures: a new inorganic host for 5-fluorouracil encapsulation. Int J Pharm. 2015;491(1–2):299–309.
12. Ouchi T, Banba T, Fujimoto M, Hamamoto S. Synthesis and antitumor activity of chitosan carrying 5-fluorouracils. Die Makromolekulare Chemie: Macromol Chem Phys. 1989;190(8):1817–25.
13. She X, Chen L, Li C, He C, He L, Kong L. Functionalization of hollow mesoporous silica nanoparticles for improved 5-FU loading. J Nanomaters. 2015;16:108–108.
14. Moodley T, Singh M. Polymeric mesoporous silica nanoparticles for enhanced delivery of 5-fluorouracil in vitro. Pharmaceutics. 2019;11(6):288.
15. Nair L, Jagadeeshan S, Nair SA, Kumar GV. Biological evaluation of 5-fluorouracil nanoparticles for cancer chemotherapy and its dependence on the carrier, PLGA. Int J Nanomed. 2011;6:1685.
16. Maney V, Singh M. The synergism of platinum-gold bimetallic Nanoconjugates enhances 5-fluorouracil delivery in vitro. Pharmaceutics. 2019;11(9):439.
17. Elmer TH. Porous and reconstructed glasses. ASM International, Engineered Materials Handbook. 1991;4:427–32.
18. Enke D, Janowski F, Schwieger W. Porous glasses in the 21st century––a short review. Microporous Mesoporous Mater. 2003;60(1–3):19–30.
19. Nordberg ME. Properties of some Vycor-brand glasses. J Am Ceramic Soc. 1944;27(10):299–305.

20. Mazilu C, Rotiu E, Ionescu L, Radu D, Dinischiotu A. Nanoporous glass in Na_2O-B_2O_3-SiO_2 oxidic system, for potential biomedical applications. J Optoelectron Adv Mater. 2007;9(7):2036–40.
21. Li S, Nguyen L, Xiong H, Wang M, Hu TC-C, She J-X, *et al.* Porous-wall hollow glass microspheres as novel potential nanocarriers for biomedical applications. Nanomed Nanotechnol Biol Med. 2010;6(1):127–36.
22. Ertuş EB, Vakifahmetoglu C, Öztürk A. Production and properties of phase separated porous glass. Ceram Int. 2020;46(4):4947–51.
23. Korsmeyer RW, Gurny R, Doelker E, Buri P, Peppas NA. Mechanisms of solute release from porous hydrophilic polymers. Int J Pharm. 1983;15(1):25–35.
24. Dash S, Murthy PN, Nath L, Chowdhury P. Kinetic modeling on drug release from controlled drug delivery systems. Acta Pol Pharm. 2010;67(3):217–23.
25. Koygun G, Arslan E, Zengin G, Orlando G, Ferrante C. Comparison of anticancer activity of Dorycnium pentaphyllum extract on MCF-7 and MCF-12A cell line: correlation with invasion and adhesion. Biomolecules. 2021;11(5):671.
26. Schüth F, Sing KSW, Weitkamp J. Handbook of porous solids. Weinheim, Germany: Wiley-Vch; 2002.
27. Dau TAN, Le VMH, Pham TKH, Le VH, Cho SK, Nguyen TNU, *et al.* Surface functionalization of doxorubicin loaded MCM-41 mesoporous silica nanoparticles by 3-aminopropyltriethoxysilane for selective anticancer 9 effect on A549 and A549/DOX cells. J Electr Mater. 2021;50(5):2932–9.
28. Enke D, Otto K, Janowski F, Heyer W, Schwieger W, Gille W. Two-phase porous silica: Mesopores inside controlled pore glasses. Journal of materials science. 2001;36(9):2349–57.
29. Thommes M, Kaneko K, Neimark AV, Olivier JP, Rodriguez-Reinoso F, Rouquerol J, *et al.* Physisorption of gases, with special reference to the evaluation of surface area and pore size distribution (IUPAC Technical Report). Pure Appl Chem. 2015;87(9–10):1051–69.
30. Šuleková M, Váhovská L, Hudák A, Žid L, Zeleňák V. A study of 5-fluorouracil desorption from mesoporous silica by RP-UHPLC. Molecules. 2019;24(7):1317.
31. El-Kady AM, Farag MM. Bioactive glass nanoparticles as a new delivery system for sustained 5-fluorouracil release: characterization and evaluation of drug release mechanism. J Nanomater. 2015;16(1):399–399.
32. Egodawatte S, Dominguez Jr S, Larsen SC. Solvent effects in the development of a drug delivery system for 5-fluorouracil using magnetic mesoporous silica nanoparticles. Microporous Mesoporous Mater. 2017;237:108–16.

How to cite this article:
Ertuş EB, Gulbahce-Mutlu E, Alpa S, Ozturk A. Production and biological properties of nano porous glass microparticles for anticancer drug carrier. J Appl Pharm Sci. 2024;14(09):120–127.